title Power Processing Unit Options for High Powered Nuclear Electric Propulsion Using MPD Thrusters
author (1) S. Krauthamer
author (2) R.S.L. Das
author (3) R.H. Frisbee
session
division Aerospace Power
abstract
An electric propulsion vehicle designed to transport cargo in support of a piloted expedition to Mars will require electrical power in the range of megawatts. This paper summarizes an evaluation of various megawatt-class power processing unit (PPU) design and technology options for high-power nuclear electric propulsion (NEP) vehicles using turboalternators and advanced magnetoplasmadynamic (MPD) thrusters. A baseline system uses a low-voltage turboalternator, rectifiers and thrusters. However, there are other options. Four such design and technology options with the potential of improving overall system efficiency and reducing cabling mass are analyzed.

The first option uses high-voltage AC from a wye-connected turboalternator and a step-down transformer, the second option uses a six-phase star-connected turboalternator instead of the wye-connected alternator in the baseline configuration, the third option uses PPU rectifier electronics located near the thrusters with a remotely-located radiator, and the fourth option uses cryogenic power conversion electronics and cabling to reduce losses.

It is found that the third option has the potential of providing maximum overall power conversion efficiency and reducing mass. Presently, the fourth option appears to have maximum complexity of design and implementation, is costly, and is somewhat uncertain even though it can be the most attractive option in the future.

IECEC 95-306

POWER PROCESSING UNIT OPTIONS FOR HIGH POWERED NUCLEAR EL. ECTRIC PROPULSION USING MPD THRUSTERS

Stanley Krauthamer
Jet Propulsion Laboratory
California Institute of Technology
Pasadena, California 91109
818-354-7740 Phone
818-393-4272 Fax

Radhe S. L. Das *
Jet Propulsion Laboratory
California Institute of Technology
Pasadena, California 91109
818-354-2453 Phone
818-393-4272 Fax

Robert H. Frisbee
Jet Propulsion Laboratory
California Institute of Technology
Pasadena, California 91109
818-354-9276 Phone
818-393-6682 Fax

ABSTRACT

An electric propulsion vehicle designed to transport cargo in support of a piloted expedition to Mars will require electrical power in the range of megawatts. This paper summarizes an evaluation of various megawatt-class power processing unit (PPU) design and technology options for high-power nuclear electric propulsion (NEP) vehicles using turboalternators and advanced magnetoplasmad ynamic (MPD) thrusters. A baseline system uses a low-voltage turboalternator, rectifiers and thrusters. However, there are other options. Four such design and technology options with the potential of improving overall system efficiency and reducing cabling mass are analyzed.

The first option uses high-voltage AC from a wye-connected turboalternator and a step-down transformer, the second option uses a six-phase star-connected turboalternator instead of the wye-connected alternator in the baseline configuration, the third option uscs PPU rectifier electronics located near the thrusters with a remotely-located radiator, and the fourth option uses cryogenic power conversion electronics and cabling to reduce losses.

It is found that the third option has the potential of providing maximum overall power conversion efficiency and reducing mass. Presently, the fourth option appears to have maximum complexity of design and implementation, is costly, and is somewhat uncertain even though it can be the most attractive option in the future.

*Also a Professor of Electrical Engineering at California State University, Long Beach, CA 90840.

INTRODUCTION

Figure 1 shows the schematic arrangement of the various components of a MW-class NEP vehicle. An electric space propulsion system consists of a power source (e.g., nuclear reactor and thermal-to-electric power conversion system). a power processing unit (PPU) which converts the power source's power output (voltage) to the form required by the thrusters, and the electric thrusters. In this study, PPUS for a 1.5 -MW_e nuclear electric propulsion (NEP) vehicle using a dynamic power conversion system (e.g., Rankine) and high-power magnetoplasmadynamic (MPD) thrusters. The baseline configuration for the NEP vehicle considered here consists of three SP-1 00 category dynamic power conversion units, a power processing module (PPM) containing the PPU electronics, and two clusters of L1-propellant MPD thrusters with 8 thrusters in each cluster.

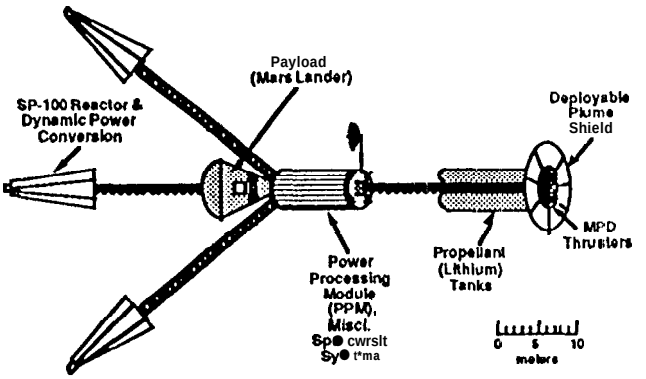

FIGURE 1. MEGAWATT-CLASS NUCLEAR ELECTRIC PROPULSION (NEP) VEHICLE WITH Li-PROPELLANT MPD THRUSTERS

Specific mass (a), expressed in units of kilograms per kilowatt of electric power (kg/kWe), and efficiency (η), expressed as the ratio of power output to power input, arc two primary figures of merit for electric propulsion systems. This study has addressed these two figures of merit.

The 1.5-MWe nuclear power system has a low-voltage (100 V), low-frequency, three-phase AC output from its dynamic power conversion system. This voltage was selected to match that required by the MPD thrusters. Thus, the output from the nuclear power system can be directly fed to a PPU rectifier for conversion to the DC voltage required by the thruster.

Li-propellant applied-field MPD thrusters were selected because of their projected good efficiency at low specific impulse (I_{sp}). Finally, the PPU for an NEP vehicle using MPD thrusters must supply different systems in the vehicle, such as thruster magnets, heaters, valves, etc., as well as general "housekeeping" power (Frisbee et al, 1993), (Das et al, 1991), (Frisbee and Hoffman, 1993).

POWER PROCESSOR UNITS FOR NEP SYSTEMS

The primary driver in PPU design in this case is a requirement of low voltage and high power. This requirement results in the use of high-ctrrrent capacity devices (e.g., 1300 to 7500 Amps). Also, the PPU must be designed to accommodate startup and shutdown transients, and be capable of isolating thruster and PPU component failures without compromising the remainder of the power or propulsion system. Thus, the PPU designs discussed below consist of both a primary high-power system and a smaller low-power power conditioning unit (PCU). For convenience, the PPU electronics components (rectifiers, filters, etc.) and switches arc treated separately from tbc component "'bus bar" wiring (both within the PPM as well as in the long booms between the PPM and thrusters or bctwccn the PPM and the nuclear power systems).

The total PPU system consists of a primary module which supplies the high-power, low-voltage DC for the thruster, and a secondary PCU module which provides the low power required by the remainder of the vehicle's systems and the thruster's components. Block schematic diagrams of PPUS for NEP systems are shown in Figures 2 and 3.

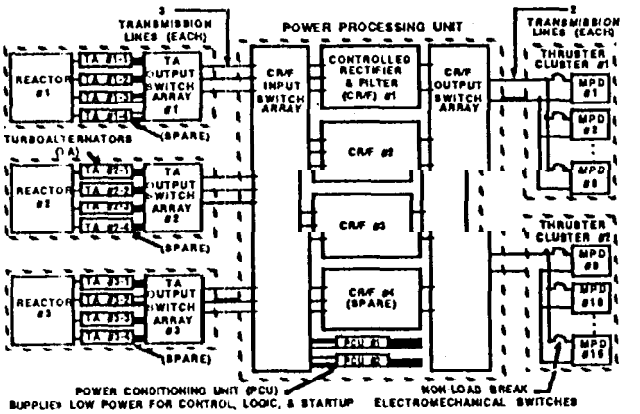

FIGURE 2. NEP-MPD PPU CIRCUIT DIAGRAM SHOWING POWER DISTRIBUTION

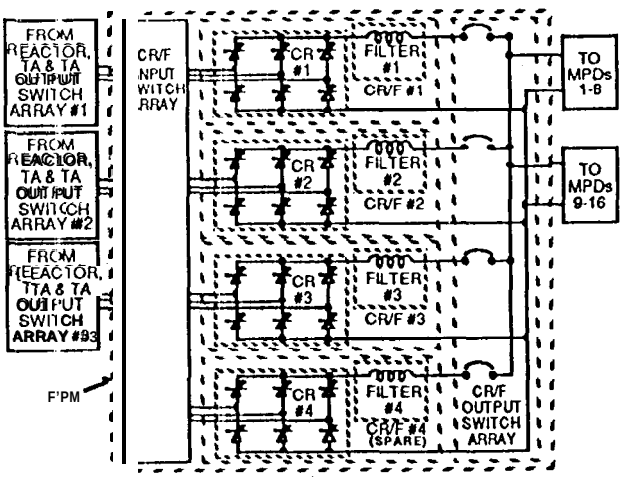

FIGURE 3. NEP-MPD PPU CIRCUIT DIAGRAM SHOWING CONTROLLED RECTIFIER AND FILTER (CR/F) CONFIGURATION

The NEP-MPD PPU consists of a multiplicity of 3-phase silicon controlled rectifiers (SCRs) or, alternatively, MOS controlled thyristors (MCTs). They receive power at 100 V AC from the turboalternators (TAs) in the dynamic nuclear power system. The SCRS are phase controlled in order to provide the variable DC voltages required to operate the MPD thrusters (Frisbee et al, 1993), (Das et al, 1991).

The switches used are non-load break type electromechanical devices that are designed to disconnect (or connect) thrusters and other components. For example, electrical power is disconnected from a thruster by first turning off the SCRs, and then by opening the non-load break thruster switch. Similarly, any of the various turboalternators or SCRs can be isolated by first driving the turboalternator voltage to zero. The TA or SCR switch can then be opened without arcing. However, the need to isolate the various components in the system does result in a complex switching topology, as illustrated in Figures 2,3,4 and 5.

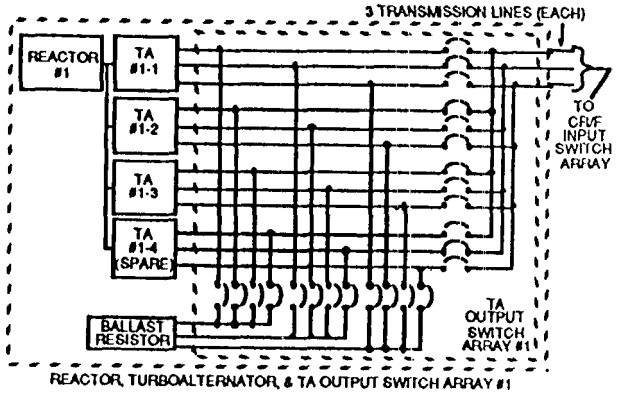

FIGURE 4. NEP-MPD PPU CIRCUIT DIAGRAM SHOWING REACTOR TURBOALTERNATOR (TA) AND BALLAST RESISTOR SWITCH CONFIGURATION (ONE OF THREE UNITS)

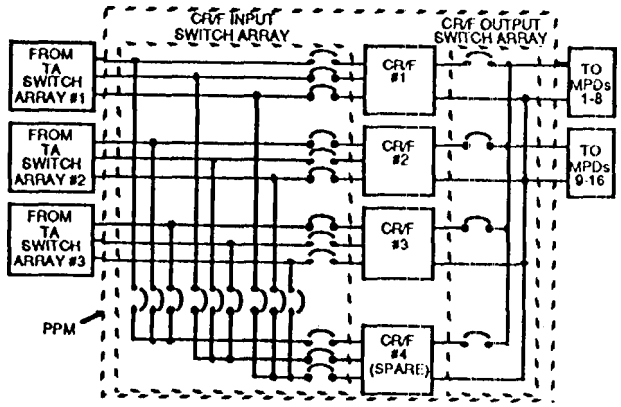

FIGURE 5. NEP-MPD PPU CIRCUIT DIAGRAM SHOWING CONTROLLED RECTIFIER/FILTER (CR/F) INPUT AND OUTPUT SWITCH CONFIGURATION

Tables 1 and 2 show a breakdown of mass, power losses, and efficiencies of various items in the baseline configuration. The overall specific mass is found to be 9.99 kg/kW_e and the overall PPU efficiently is about 90.0%.

TABLE 1. POWER CONDITIONING MASSES AND EFFICIENCIES

ITEM	QUANTITY	TOTAL MASS (kg)	TOTAL LOSSES (kW)	COMMENTS
Turboalternator (TA) Switches (100 VAC, 1333 A)	36	245	1.5	Sum of all Switches
TA Ballast Switches (100 VAC, 3300 A)	26	734		
CR Input Switches (100 VAC, 3300 A)	21	430		
Controlled Rectifiers (CR) (100 VAC, 5000 A)	4	13s	40.0	25°C coolant temp
Output Chokes (Filters, F) (100 VDC, 5000 A)	4	m	3.0	25°C coolant temp.
CR/F Output Switches (100 VDC, 5000 A)	4	114		
Thruster Switches (100 VDC, 7500 A)	16	454		
House-keeping Pcu	2	344	3.0	63 kWe h, 60 kWo out PCU has its own radiator
Structure		100		
Radiator		931	(44.5)	Total PPU radiator load
Tow		3773	107.5	PCU input counted as loss

TABLE 2. CABLE AND BOOM MASSES AND EFFICIENCIES

ITEM	NO. OF CABLES	LENGTH EACH (m)	CURRENT EACH (A)	TOTAL MASS (kg)	TOTAL LOSSES (kW)
Reactor Booms					
TA-to TA Switch	36	2 2	1100	605	0 6
TA Parallel Connections	9	1.5	1100	103	0 2
TA-to Ballast Resistor Switch	36	1.s	1100	412	0 6
Ballast Resistor Parallel Connections	9	2.2	3300	269	1.2
Reactor Boom	6	24.0	3300	2931	1 2 9
Docking Connectors	18	o 2s	3300	90	2 0
Structure (25 %)				1103	
Subtotal				5,513	17.6
PPM Cabling					
Input to-Switch-to-CR	12	2.2	3300	358	1.6
Input-to-Spare CR Switches	9	0.9	3300	110	0.5
Controlled Rectifier (CR) Internal	12	0.9	3300	147	0.6
CR-to Filter-to-Switch-to-Output		0.5	5000	122	0.2
Output Parallel Connections	:	2.0	7500	122	0.6
Structure (25%)				215	
Subtotal				1,074	3.5
Thruster Cluster (TC) Booms					
PPM to TC Boom	4	20.0	7500	2079	165
TC Boom	4	2.0	7500	244	1.1
TC Connections	4	2.5	7503	376	1.1
Structure (25%)				925	
Subtotal				4.626	21.7

THE RATIONALE BEHIND THE PPU OPTIONS

The following factors influence the selection of a PPU option:

1. PPU and cabling mass
2. PPU efficiency
3. PPU redundancy so that each thruster dots not have a dedicated PPU
4. PPU thermal control

Four PPU options have been considered in this paper. The block schematic diagram in Figure 6a represents the baseline system while Figures 6b, 6c, 6d, and 6c represent these four options. Option I uses high-voltage (7500 VAC) turboalternators (TAs) and step-down transformers (to reduce the voltage to the 100 VDC required by the thrusters) to reduce TA-to-PPM line losses. Option II uses low-voltage turboalternators with six-phase "star" windings (instead of the "wye" windings in the baseline design) to reduce the number of rectifiers by one-half, and thus reduce rectifier mass and power losses. Option III uses high-voltage TAs like

Option I but locates the PPM electronics (step-down transformers, rectifiers, filters, etc.) near the thrusters to reduce PPM-to-thruster line 1o SSCS. However, this requires a remotely-located PPM radiator because, in all of these designs, the waste-heat radiator for the PPU electronics must be located at least 30 m from the thrusters (to minimize thruster Li-propellant plume impingement and coating of the radiator), and at least 24 m from the reactors (to minimize radiation effects). Option IV uses a configuration similar to the baseline system but with cryogenic cooling of PJ'U components, such as cryogenic MOSFET rectifiers (instead of room-temperature MCTS or SCRs) and high-temperature superconducting cables, to reduce PPU losses.

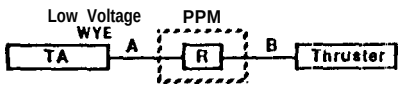

FIGURE 6a. BASELINE SYSTEM BLOCK SCHEMATIC DIAGRAM

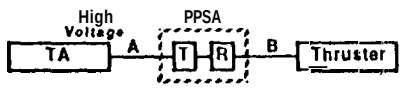

FIGURE 6b. OPTION 1 BLOCK SCHEMATIC DIAGRAM

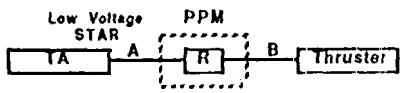

FIGURE 6c. OPTION II BLOCK SCHEMATIC DIAGRAM

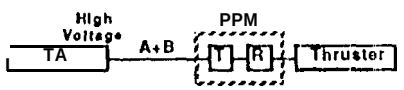

FIGURE 6d. OPTION III BLOCK SCHEMATIC DIAGRAM

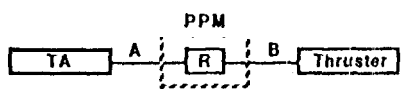

FIGURE 6e. OPTION IV BLOCK SCHEMATIC DIAGRAM

A = TA-to-PPM Boom & Cables R = Rectifier
B = PPM-to-Thrusters Boom T = Transformer
● Cables

FIGURE 6. BLOCK SCHEMATIC DIAGRAMS FOR BASELINE CONFIGURATIONS AND OTHER OPTIONS

The rationale behind these options is as follows. Option I has the advantage of *reducing* the mass of cabling from the turboalternators to the PPM. However, this option introduces additional mass and 1osscs due to the step-down transformer. Option Il has the advantage of requiring a smaller number of rectifiers (e.g., one-half the number required for a "wye" configuration) with a potential reduction in rectifier mass and losses. However, increases in mass due to the increased number of cables in the long turboalternator-to-PPM boom must also be considered. Option III has the advantage of reducing the length of the low-voltage DC cables. As shown below, this option holds the promise of dramatically reducing the total mass and losses in the long thruster boom cables. However, this option requires a mechanically complex and potentially power-intensive pumped-fluid loop cooling system whose impact must be included. In Option IV, it is assumed possible to passively cool the various components to 77 K (with minimal additional active liquid nitrogen cooling) by designing a system with minimum heat leaks from the "warm" spacecraft, and by maintaining a view of deep space rather than of a planet or the sun. Its potential advantage is a dramatic improvement in efficiency combined with a potential reduction in size, weight and cost because there is *no* heat sink, pomp, or isolation requirement.

POWER LOSS, EFFICIENCY, AND MASS CALCULATIONS

Power loss (P_{loss}) and efficiency (η) of any component are related by the equations:

$$\eta = (\text{Output Power})/(\text{input Power})$$
$$P_{loss} = (1-\eta) \cdot (\text{input Power})$$

Table 3 shows calculated values of power losses and efficiencies in each option along with their specific mass. In calculating the radiator area (A) and mass (m), the following equations have been used:

$$A\ (m^2) = (\text{Power Loss, Watts})/\ K \cdot T^4 \cdot \varepsilon$$
$$m\ (\text{kg}) = A \cdot w \cdot CF$$

where

K = Stefan Boltzman Constant = $5.67 \times 10^{-8}\ W/m^2K^4$
& = Emissivity (0.8)
T = Temperature (Kelvin) = 298.15 K in the baseline design
w = Radiator Areal Density (5 kg/m^2)
CF = Contingency Factor (1.5)

In the baseline configuration, the current is high throughout because of low voltage. As a result, these cables are thicker and they also provide strength and integrity to the boom structure. The power losses in cables A and B are 18 kW and 22 kW, respectively. The power loss in PPU electronics is 108 kW. The total PPU mass is about 14,986 kg out of which the mass of all cabling and booms is 11,213 kg. The mass of cable in section A is 5513 kg and in section J? is 4626 kg. The PPM electronics and radiator weighs about 3773 kg. The ovei all efficiency and specific mass are calculated to be 90.0% and 9.99 kg/kW_e, respectively. Finally, note that the "housekeeping" PCU power, 63 kW, is considered a "loss" in determining PPU efficiency because this power is unavailable for usc by the MPD thrusters.

In the Option I configuration, the cable mass and power loss in section B arc the same as those in baseline configuration. However, the current in section A in smaller duc to higher voltage (e.g., 7500 VAC versus 100 VAC for the baseline). It is found that the power loss in this section is about 2/75th of the baseline loss, or about 0.5 kW. The cable mass in section A is estimated to be l/75th of baseline cable mass plus 10% to allow for interconnections and higher switch masses. As a result, the total PCU, electronics, and cable power loss is 133.2 kW. Assuming transformer efficiency to bc 99.7% throughout, the power loss in transformers is 4.5 kW. Therefore, the overall efficiency is 90.89.. The total transformer mass is estimated to be 227 kg. The transformer waste-heat radiator mass at 150°C is negligible (68 kg). Therefore, the specific mass in the Option I configuration is 6.57 kg/kW_e.

In the Option II configuration, the cable mass and power loss in the section B cables remain unchanged. In the section A cables, the RMS value of input current is 0.577 times the required DC current of the baseline three-wire wye - connection. and is 0.408 times the required DC current in the six-wire star connection. As a result, the RMS current in this option is 0.707 times the current in the baseline design. The cable power loss in section A is found to be 1.414 times the loss in the baseline case. Similarly, the cable mass in section A is 1.414 times that in the baseline design. In fact, the mass increase in the section A cables completely outweighs the savings in rectifier mass made possible by the "star" configuration. Interestingly, this option does have an overall efficiency comparable to that of Option 1, but with a significant increase in total specific mass.

In (hc Option III configuration, the transformer and electronics are located near the thrusters. As a result, the high-voltage TA-to-PPM cables will have a total power loss of approximately 1 kW. The power loss in the transformer is again estimated to be 4.5 kW. A power loss of 2.2 kW is allocated to the low-voltage cables within the thruster clusters. The total mass of high-voltage cables (A + B) is estimated to be l/75th of the total mass of the baseline cables (A + B) plus 10% for connectors. In this case, the high-voltage cables (A + B) mass and power savings easily compensate for the added mass and power rcqu ired for the pumped-fluid loop for the PPM electronics waste-heat radiator.

Finally, in the Option IV configuration, the room-temperature SCR or MCT rectifiers are replaced with ultra-high efficiency cryogenic MOSFET rectifiers. The mass and power loss in both cables A and B, without cryogenic cooling of cables, remains the same as in the baseline. configuration. The mass of a cryogenic refrigeration system would however have to bc considered, but in this case, the mass of conventional cables is so high that the impact of a refrigeration system will be minimal. Also, the mass of other items such as heat sink or isolation requirement is minimum. Assuming an efficiency of 99.5% (Muller and Herd, 1993) for ultra-high efficiency cryogenic MOSFETs, the power 1ossCs in a cryogenic power conversion unit would bc 7.5 kW plus 4.5 kW for the room-temperature switches, filters, etc. As a result, the total PPU system power loss (including PCU and conventional room-temperature cables) is 118 kW, and the overall efficiency would be about 92.1%. The specific mass would have a value in the range of 10.9 kg/kW_e. Interestingly. if the cables were assumed to be cryogenically cooled high-temperature (77 K) superconductors, there could be a significant improvement in efficiency because the total power loss of 43 kW in cables of the baseline design would be eliminated. This would result in an overall efficiency of 95.3%. ALso, there could be an improvement in specific mass due to a reduction in cable mass. (In the baseline option, the cables are heavy because of a need for a large cross-sectional area to reduce resistive losses; by contrast, a superconducting cable with the same current carrying capacity could be made much thinner and lighter.) However, it is not known at this time what mass impacts would be associated with the thermal insulation and cooling required for superconducting cables.

TABLE 3. COMPARISON OF MASS, TOTAL POWER LOSS, EFFICIENCY, AND SPECIFIC MASS FOR VARIOUS OPTIONS

OPTION	TOTAL MASS (kg)	TOTAL POWER LOSS (kW)	EFFICIENCY (%)	SPECIFIC MASS* (kg/kW_e)
Baseline	4,986	50.5	90.0	9.99
Option I	9,849	37.7	90.8	6.57
Option II	6,782	37.9	90.8	11.19
Option III	6,815	18.7	92.1	4.54
Option IV	16,306	118.0	92.1	10.87

•Nominal input power= 1500 kW.

Based on the values of efficiency and specific mass associated with each option shown in Table 3, Options I and III, which both employ high-voltage (7500 VAC) turboaltemators to reduce the mass and power losses of the TA-to-PPM cables, provide significant improvements over the baseline system, with Option III showing the greatest benefits. Option II, which employs a "star" TA winding, is inferior to the baseline system's "wye" TA windings due to increased cabling mass. Finally, Option IV, which uses ultra-high efficiency power conversion with cryogenic MOSFETs, can provide significant improvements in efficiency at the cost of only a slight increase in system specific mass. Further improvements could bc realized with the usc of high-temperature (77 K) superconducting cables.

CONCLUSIONS

Based on the comparison value.s shown in Table 3, one can make the following conclusions:

1. Option 111, which employs high-voltage TAs and a PPM located near the thrusters, holds the maximum promise for dramatic reductions of total mass and power loss. However, this option does present some mechanical complexity in requiring a pumped-fluid loop cooling for a remotely-located radiator,

2. Option IV, which employs cryogenic. ultra-high efficiency power conversion, is attractive if its complexity of design or implementations can be **reduced.** For example, the impacts on spacecraft design, configuration, reliability, and operations (e.g., keeping the cryogenic systems pointed "away" from the sun to minimize active refrigeration requirements) arc not known. At present, the uncertainty and complexity associated with this option make it less attractive than Option 111. It is recommended that Option IV be addressed in additional detail in future studies to assess the benefits that could be realized from a cryogenic PPU system employing cryogenic rectifiers and superconductors. with special emphasis on rcccnt advances in high-temperature superconductor technology because of the significant improvements in system efficiency that this technology may enable.

ACKNOWLEDGMENTS

The work dcscribcd in the paper was performed by the Jet Propulsion Laboratory, California Institute of Technology, under contract with the National Aeronautics and Space Administration.

REFERENCES

Frisbee, R.H., Das, R. S. L., and Krauthamer, S., Sept. 13-16, 1993, "Power Processing Units for High Powered Nuclear Electric Propulsion with MPD Thrusters," 23rd International Electric Propulsion Conference, Seattle, WA.

Das, R.S.L, Krauthamer, S., Frisbee, R.H., and McGee, D. P., Sept. 4-6, 1991, "Power Processing Units for High Powered Nuclear Electric Propulsion,* AIAA/NASA/OAI Conference on Advanced SEI Technologies, Cleveland, OH.

Frisbee, R. and Hoffman, N., June 28-30, 1993, "SP-l 00 Nuclear Electric Propulsion for Mars Cargo Missions," AIAA/SAE/ASME/ASEE 29th Joint Propulsion Con ference and Exhibit, Monterey, CA.

Muller, O.M. and Herd, K.G., 1993, "Ultra-High Efficiency Power Conversion Using Cryogenic MOSFETs and HT-Superconductors," 0-7803 -1243 -0/93 S03.00 IEEE.